JOURNAL OF COMPUTATIONAL PHYSICS 19, 267–279 (1975)

Mass Tensor Molecular Dynamics

CHARLES H. BENNETT*

IBM Thomas J. Watson Research Center, Yorktown Heights, New York 10598

Received March 20, 1975

If one replaces the ordinary kinetic energy function for a classical system of point masses ($\frac{1}{2}\sum_{i=1}^{N} m_i\dot{q}_i^2$) by a more general quadratic form ($\frac{1}{2}\sum_{ij=1}^{N} \dot{q}_i M_{ij}\dot{q}_j$), where M_{ij} is an arbitrary positive-definite symmetric "mass tensor," one obtains a system having different dynamics but the same equilibrium properties as the original system. By appropriate choice of M_{ij}, high frequency motions can be slowed down and low frequency ones speeded up, thereby increasing the efficiency with which configuration space can be explored in a given amont of computer time. Tests of the method on a short Lennard–Jones polymer chain indicate that a five- to tenfold saving of computer time is possible for such systems.

I. INTRODUCTION

The molecular dynamics method is typically applied to a system of mass points ("atoms") describable by a classical Hamiltonian

$$H = \tfrac{1}{2}\sum_{i=1}^{N} m_i\dot{q}_i^2 + U(q_1 \cdots q_N), \tag{1}$$

where q_i is the ith Cartesian coordinate, m_i its mass, and U the potential energy. The equilibrium properties of such a system (as opposed to its transport or relaxation properties) are independent of the kinetic part of the Hamiltonian, and could just as well be studied in a system whose kinetic energy was a more general quadratic function of the velocities, e.g.,

$$H' = \tfrac{1}{2}\sum_{ij=1}^{N} \dot{q}_i M_{ij}\dot{q}_j + U(q_1 \cdots q_N), \tag{2}$$

or, in a more compact notation,

$$H' = \tfrac{1}{2}\dot{\mathbf{q}}^T\mathbf{M}\dot{\mathbf{q}} + U(\mathbf{q}) \tag{3}$$

* Work begun at the Centre Européen de Calcul Atomique et Moléculaire, Université de Paris Bâtiment 506, 91 Orsay France and continued at IBM Research Center.

where **M**, the "mass tensor," is an arbitrary positive-definite N by N symmetric matrix. Newton's equations of motion for the new system are then

$$\ddot{\mathbf{q}} = -\mathbf{M}^{-1}\nabla U(\mathbf{q}). \tag{4}$$

The goal of doing dynamics on such an artificial system would be, by judicious choice of the mass tensor, to slow down the original system's high frequency motions and speed up its low frequency motions, thereby making possible a more efficient sampling of the system's configuration space in a given amount of computer time. For the mass tensor method to be worthwhile, the gain in sampling efficiency must more than offset the extra computational work involved in computing the accelerations from the forces by Eq. (4). Typically this requires about as much time as the force calculation, which also must be done once per time step.

Information on the local shape of the potential energy surface in configuration space, and hence on the local oscillation frequencies, can be obtained from the instantaneous matrix of force constants:

$$A_{ij}(\mathbf{q}) \equiv \partial^2 U(\mathbf{q})/(\partial q_i\, \partial q_j). \tag{5}$$

If the system is nearly harmonic (e.g., a low temperature crystal or glass) the **A** matrix will be approximately constant throughout the accessible portion of configuration space, and the oscillation frequencies can all be made approximately equal by taking

$$\mathbf{M} = \mathbf{A} \cdot \text{const}, \tag{6}$$

where the **A** matrix has been evaluated at a fixed but arbitrary configuration not too far from the configuration of minimum energy. The normalization constant is arbitrary, but may conveniently be taken to be $|\mathbf{A}|^{-1/N}$. When Eq. (6) is used to define the mass tensor, mass tensor dynamics becomes analogous to quadratically convergent methods of function minimization [1, 2]. These, by taking advantage of local curvature information, avoid the excessive oscillation characteristic of steepest-descent methods. Of course the goal of function minimization (to find the local minimum quickly) is different from that of dynamics (to explore the low-energy part of the potential surface quickly, but in a statistically representative manner).

Unfortunately, in the strongly anharmonic systems in which one is typically interested (e.g., liquids; polymers capable of undergoing conformational rearrangement), the **A** matrix is neither approximately constant nor positive definite [3], and there is no obvious "best" choice for the mass tensor. The approach that will be used in the present study is to define the mass tensor as a matrix having the

same eigenvectors as a typical instantaneous or time-averaged **A** matrix, but a different set of eigenvalues, all positive; i.e.,

$$M_{ij} = \sum_k V_{ik} f(\lambda_k)\, V_{jk} \cdot \prod_k f(\lambda_k)^{-1/N}, \tag{7}$$

with λ_k being the eigenvalues and **V** the orthogonal matrix of column eigenvectors of **A**. The function f, which must always be positive, is empirically chosen so as to roughly equalize the system's local oscillation frequencies, some of which are rather ill-defined.

Before attempting to apply the mass tensor method, an exploratory study was made of the relation between the eigenvalue spectrum of **A** and the local shape of the potential energy surface in two typical anharmonic systems:

(1) a free droplet of 24 atoms interacting via the Lennard–Jones pair potential,

$$u(r) = 4\epsilon[(\sigma/r)^{12} - (\sigma/r)^6]; \tag{8}$$

(2) a 10-atom flexible polymer chain with harmonic forces between bonded atoms (bond length $= 0.7071\sigma$, force constant $= 30000\epsilon/\sigma^2$) and Lennard–Jones forces between all other, nonbonded pairs of atoms. The ratio of bonded to nonbonded forces in this system is of the same order of magnitude as that found in organic polymers.

The next section describes the results of the eigenvalue study, while the Section III describes the application of mass tensor dynamics to the polymer chain system. Section IV discusses the dynamics of systems in which the mass tensor is not constant.

II. Eigenvalues of the A Matrix and the Shape of the Potential Energy Surface

Figure 1 shows the distribution of eigenvalues of the **A** matrix observed in two configurations of the 24-atom droplet, one occurring during a run corresponding to argon at 20 K (upper histogram); the other during a run at 35 K (lower histogram). The three zero-frequency eigenvalues corresponding to pure translations are omitted from the histograms (because the droplet is vibrationally excited, the three rotational degrees of freedom mix with the vibrational degrees of freedom and do not give rise to any further zero eigenvalues). The most noteworthy features of the spectra are the presence of negative eigenvalues (characteristic of anharmonicity) which become much more numerous as the temperature is increased, and

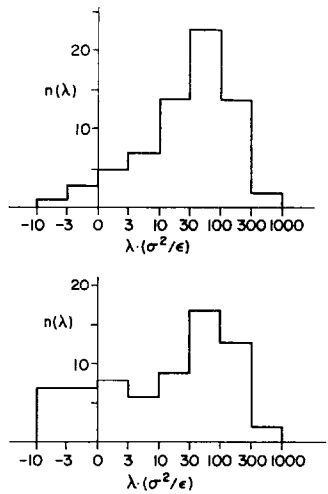

FIG. 1. Eigenvalue spectra of the instantaneous force constant matrix for a 24-atom Lennard–Jones droplet at two temperatures: top curve—conditions comparable to argon at 20 K ($E = -84.6\epsilon$, $kT/\epsilon = 0.16$); bottom curve—conditions comparable to argon at 35 K ($E = -70.2\epsilon$, $kT/\epsilon = 0.29$).

the overall width of the spectrum, with most positive eigenvalues falling between 10 and 300. This 30-fold spread of eigenvalues implies only a $(30)^{1/2}$-fold spread of normal mode frequencies; hence the droplet is unlikely to show much improvement on going from normal to mass tensor dynamics. For this reason the remaining tests were conducted on the flexible polymer chain, which has a much broader eigenvalue spectrum (cf. Fig. 2).

The polymer chain was started in a helical configuration at a temperature $kT/\epsilon = 0.83$, corresponding to 100 K, and allowed to move according to the two-body forces already described. In order to destroy the system's translational and rotational symmetry, one-body harmonic restoring forces (force constant $30000\epsilon/\sigma^2$) were applied to the x, y, and z coordinates of atom 1, the x and y coordinates of atom 2, and the x coordinate of atom 3. The **A** matrix therefore had no zero eigenvalues. The upper histogram in Fig. 2 is the average of ten instantaneous eigenvalue spectra taken at different times during a run. The distribution of positive eigenvalues varied very little from one configuration to the next, but the number of negative eigenvalues varied from two to seven. The variability of the negative eigenvalues, as well as the suprisingly high absolute values of some of them, suggests that they represent rather localized convex wrinkles on a generally concave potential energy surface. This hypothesis is confirmed by the fact that if the various second derivatives of U are averaged over a few hundred steps of ordinary dynamics, rather than being computed for a single configuration, the

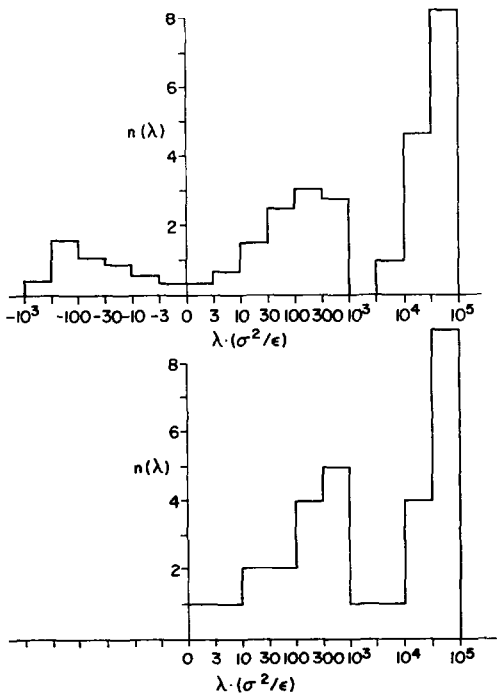

FIG. 2. Eigenvalue spectra of the 10-atom flexible polymer chain under conditions comparable to argon at 100 K ($E = -2.5\epsilon$, $kT/\epsilon = 0.83$). Upper curve—instantaneous eigenvalue spectrum; lower curve—eigenvalue spectrum of a force constant matrix averaged over 269 steps of normal dynamics (elapsed time 0.55 $(m\sigma^2/\epsilon)^{1/2}$).

resulting time-averaged **A** matrix, $\bar{\mathbf{A}}$, has no negative eigenvalues (lower curve in Fig. 2).

In order to better understand the relation between the eigenvalue spectrum and the shape of the potential surface, a typical polymer configuration was selected, its instantaneous **A** matrix was evaluated and diagonalized, and the normal coordinates $Q_1, Q_2, \ldots, Q_N$ were defined as

$$Q_j = \sum_i q_i V_{ij}, \tag{9}$$

where V_{ij} is the orthogonal matrix of column eigenvectors of **A**. For each Q_j, a cross section of the potential surface in the Q_j direction was prepared by observing the variation of the potential energy as that normal coordinate was varied while all others were kept fixed. Four such cross sections are shown in Fig. 3; in each case the point $\Delta Q = 0$ corresponds to the reference configuration at which **A** was evaluated, and with respect to which energy differences ΔU are measured.

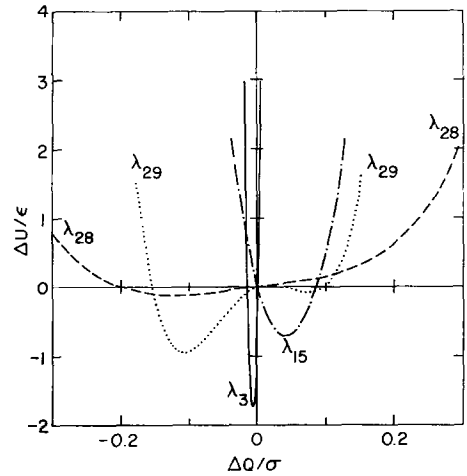

FIG. 3. Cross sections of the potential energy surface along principal axes of the force constan matrix, for a typical instantaneous configuration of the 10-atom polymer chain. Four cross sections are shown, corresponding to the eigenvalues $\lambda_3 = 44000$, $\lambda_{15} = 660$, $\lambda_{28} = 1.7$, and $\lambda_{29} = -122$, all in units of ϵ/σ^2.

The cross sections corresponding to the larger positive eigenvalues, e.g., $\lambda_3 = 44000$ and $\lambda_{15} = 660$, were approximately parabolic, with width proportional to $1/(\lambda)^{1/2}$. The cross sections corresponding to the smaller positive and the negative eigenvalues (e.g., $\lambda_2 \cdot = 1.7$ and $\lambda_{29} = -122$) were flat- or convex-bottomed, steep-sided valleys ranging in width between 0.3σ and 0.7σ, i.e., no wider than a harmonic valley of curvature 10. For this reason the dynamical tests described in the next section were conducted with the f function

$$f(\lambda) = \max\{10, \lambda\}. \tag{10}$$

Also, because of the apparent transience of the negative eigenvalues, the eigenvalues λ_k and eigenvectors V_{ij} were obtained from a time-averaged, rather than an instaneous, **A** matrix. Since time-averaging obliterates the negative eigenvalues, the only effect of the f function was to harden the few lowest positive eigenvalues relative to the others. A rather similar result could have been achieved without diagonalizing the averaged **A** matrix at all, merely by adding 10 to all its diagonal elements,

$$M_{ij} = (\bar{A}_{ij} + 10\delta_{ij}) \cdot \text{const.} \tag{11}$$

Although this would have increased *all* the eigenvalues by 10, the effect on the oscillation frequencies corresponding to the larger positive eigenvalues would have been negligible.

III. Trials of Mass Tensor Dynamics

Given a potential energy function $U(\mathbf{q})$ and a mass tensor $\mathbf{M}$, Newton's equations of motion (Eq. (4)) can be solved in several ways:

(1) The positions, velocities, and accelerations can all be expressed, and Eq. (4) integrated, in normal coordinates Q_i, $\dot{Q}_i$, $\ddot{Q}_i$, with respect to which $\mathbf{M}$ is diagonal (cf. Eq. (9)).

(2) The inverse of $\mathbf{M}$ can be calculated and used to integrate Eq. (4) directly in atomic coordinates, the forces being multiplied by $\mathbf{M}^{-1}$ to obtain the accelerations $\ddot{q}_i$.

(3) $\mathbf{M}$ can be factored into the form $\mathbf{M} = \mathbf{PLDL}^T\mathbf{P}^T$ where $\mathbf{P}$ is a permutation, $\mathbf{D}$ a diagonal, and $\mathbf{L}$ a lower triangular matrix with ones on the diagonal. Newton's equation

$$\mathbf{PLDL}^T\mathbf{P}^T\ddot{\mathbf{q}} = -\nabla U(\mathbf{q}) \tag{12}$$

is then back-solved for the atomic accelerations $\ddot{\mathbf{q}}$ at each time step.

Method 1 is relatively wasteful of computer time because it requires diagonalizing the mass tensor initially, and, at each time step, transforming back and forth between atomic and normal coordinates, since the function ∇U can only be computed in the atomic basis. Nevertheless this method was used in the numerical work to be described below, because the machinery for generating and using the transformation matrix $\mathbf{V}$ was already available as a result of the energy surface cross section studies. Method 2 is the most straightforward, does not require a diagonalized mass tensor (thus allowing the mass tensor to be defined in terms of a nondiagonalized force constant matrix, as suggested by Eq. (11)), and requires only one matrix–vector multiplication per time step, as opposed to two for method 1. However, for systems with a large number of degrees of freedom, method 3 is probably the best because, while retaining the advantages of method 2, it allows sparse matrix techniques [4, 5][1] to be used to advantage. When the dimensions of the system being studied are large compared to the range of interatomic forces, most elements of the force constant matrix, and hence of the mass tensor, will be zero. In general, all this sparsity will be lost in the inverse mass tensor $\mathbf{M}^{-1}$, used in method 2; however, much of it can be retained in the triangular matrix $\mathbf{L}$ of method 3, by appropriate choice of the permutation $\mathbf{P}$ [6].[2] Preservation

[1] See in particular the summary paper by F. G. Gustavson in [5].

[2] This paper discusses regular arrays of objects (e.g., atoms), with short-range interactions; however, its results can presumably be generalized to dense, irregular arrays. When the size of a three-dimensional array is large compared to the range of interaction, the number of nonzero elements in the $\mathbf{L}$ matrix can be made to increase as the 4/3 power of N, by an appropriate permutation strategy (cf. p. 358).

of sparsity is important because the time required to compute the accelerations from the forces at each time step is proportional the number of nonzero elements in $\mathbf{M}^{-1}$ (for method 2) or in $\mathbf{L}$ (for method 3).

The comparison of ordinary and mass tensor dynamics was carried out on the ten-atom polymer chain described in the last paragraph of Section I and the second paragraph of Section II. For both ordinary and mass tensor dynamics the equations of motion (including the symmetry-destroying one-body forces) were integrated by a five-derivative Gear algorithm [7, 8],[3] the algorithm being applied to the atomic coordinates and their time derivatives for the ordinary runs and to the normal coordinates and their time derivatives for the mass tensor runs. The time step Δt was automatically adjusted to hold the total energy within $\pm 0.5\epsilon$ of its nominal value for about ten time steps. Whenever the energy drifted out of bounds, the system was restarted from its previous configuration with a new Maxwellian set of velocities, scaled so as to restore the energy to its nominal value of -2.5ϵ (the mean energy, -2.3ϵ, consisted of 12.2ϵ kinetic and -14.5ϵ potential energy).

To define the mass tensor, the force constants were averaged over an ordinary dynamics run of 269 steps. The resulting matrix $\bar{\mathbf{A}}$ was then diagonalized to obtain its eigenvalues λ_k (cf. lower histogram in Fig. 2) and eigenvectors V_{ij}, and the mass tensor was defined by Eq. (7) using the f function of Eq. (10) (this merely had the effect of increasing to $+10$ the $\bar{\mathbf{A}}$ matrix's two softest eigenvalues, namely, $+1.7$ and $+5.4$). The run was then continued for about 6000 steps of mass tensor dynamics, using the mass tensor calculated in the first 269 steps. A 3000-step ordinary dynamics run from the same starting configuration was made for comparison.

Assessment of the relative efficiency of ordinary and mass tensor dynamics in exploring configuration space is a somewhat subtle problem. The maximum time step Δt tolerated by the integration algorithm is not a good criterion, because the definition of the mass tensor (cf. Eq. (6)) introduces an arbitrary normalization factor in the time. In the present work, where the normalization convention of Eq. (7) was used, some modes were speeded up and others slowed down, but the maximum time step for mass tensor dynamics remained about the same as for ordinary dynamics, about 0.002 $(m\sigma^2/\epsilon)^{1/2}$. Two better measures of efficient dynamics are: (1) the squared end-to-end distance, $(\mathbf{r}_{10} - \mathbf{r}_1)^2$, as a function of elapsed number of time steps; and (2) the mean squared displacement in configuration space in n time steps,

[3] The following timing information (for the IBM 360-91 computer, Fortran H optimizing compiler) may be of interest. One time step of ordinary dynamics = 1.4 msec (mostly in force calculation); one time step of mass tensor dynamics = 3.0 msec; diagonalization of force constant matrix (double precision) = 1000 msec.

$$S_n \equiv \left\langle \sum_{i=1}^{N} [q_i(t + n\,\Delta t) - q_i(t)]^2 \right\rangle, \tag{13}$$

as a function of n. In order for S_n to be a reliable measure of conformational change, the system must be prevented from undergoing rotational or translational drift. This was the principal purpose for the one-body forces on the first three atoms of the chain.

As Fig. 4 shows, the end-to-end distance fluctuates about as much in 100 steps

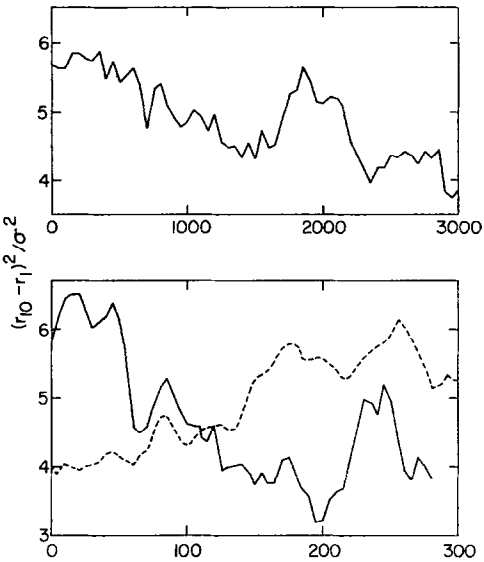

FIG. 4. Squared end-to-end distance, as a function of elapsed number of time steps (abscissa—note scale difference between upper and lower graphs). Upper solid curve: normal dynamics run; lower solid curve: initial portion of mass tensor run, immediately after calculation of mass tensor; lower dashed curve: end of mass tensor run, beginning 5430 time steps after calculation of mass tensor.

of mass tensor dynamics as in 1000 steps of ordinary dynamics. Although the chain did not undergo a major conformational change (i.e., it remained a left-handed helix throughout even the 6000-step mass tensor run), it appears likely that major as well as minor confirmational changes would occur much sooner under mass tensor than under ordinary dynamics. The persistence of fairly rapid fluctuations at the end of the mass tensor run (dashed curve) shows that the local curvature information gathered at the beginning of the run did not rapidly become obsolete.

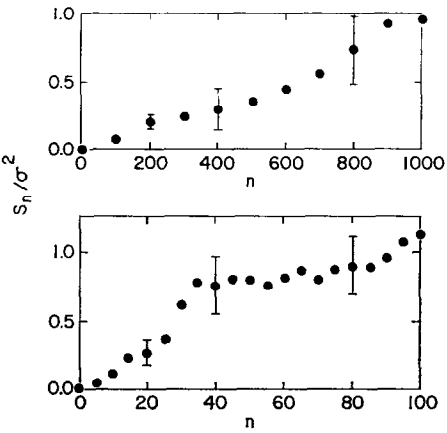

FIG. 5. Diffusion parameter S_n as a function of elapsed number of time steps n (note scale difference between upper and lower abscissa). Upper graph: average over three time origins in normal dynamics run; lower graph: average over five time origins in mass tensor run. Bars show typical standard errors of the plotted means.

The increase of S_n with n measures the system's diffusion away from its original configuration. As Fig. 5 shows, this also occurred about ten times more rapidly under mass tensor dynamics than under ordinary dynamics. In both the runs, S_n leveled off at about $2\sigma^2$ at long times, which indicated that the system was trapped in a relatively small region in configuration space corresponding to the left handed helical conformation. The rms length of a single dynamical step in configuration space, $(S_1)^{1/2}$, was about 0.01σ under ordinary dynamics and about 0.05σ under mass tensor dynamics.

All these results indicate that the mass tensor method accomplishes about ten times as much configurational change per time step as ordinary dynamics, or about five times as much per second of computer time. A more dramatic improvement could be expected in a system having a greater disparity between its hard and soft modes.

The failure of the 10-atom chain to undergo a major conformational transition, even with the assistance of mass tensor dynamics, emphasizes the distinction between events that are infrequent primarily because they involve soft, slowly relaxing degrees of freedom and events whose infrequency results primarily from the presence of a large activation barrier. Events of the latter type need not be associated with any particularly soft modes of the force constant matrix, and may remain quite infrequent under mass tensor dynamics. Such events are probably best studied by molecular dynamics and Monte Carlo methods [9][4] in which an

[4] Section II-4 and Appendix B of [9] discuss the application of saddle point methods to vacancy jumps in a crystal.

artificial constraint force is used to push the system into the relevant saddle point neighborhood in configuration space (unfortunately these methods can only be used when the approximate saddle point is known). Chirality reversal of the 10-atom chain is probably an infrequent event of intermediate type. On the one hand it probably involves degrees of freedom which relax about as slowly as the end-to-end distance. On the other hand, there is a sizable activation barrier because of the need to simultaneously disrupt most of the Lennard–Jones bonds available in the helical conformations, in order to get from one to the other.

IV. Nonconstant Mass Tensors

This section generalizes the mass tensor by allowing it to be a function of the coordinates $\mathbf{q} \equiv (q_1 \cdots q_N)$, rather than a constant matrix as has been assumed up to now. Thereafter, some attention will be given to the problem of whether a nonconstant mass tensor must be "memoryless" (i.e., be a function of the present configuration only) to sample configuration space correctly.

One reason for allowing the mass tensor to be a function of $\mathbf{q}$ is to enable the mass tensor method to be extended to systems (such as a system of rigid-body molecules described by center-of-mass cartesian coordinates and Euler angles) whose kinetic energy is inherently a function of both $\mathbf{q}$ and $\dot{\mathbf{q}}$. Even the ordinary dynamics of such a system requires a Hamiltonian of the form

$$H = \tfrac{1}{2} \sum_{ij} \dot{q}_i M_{ij}(\mathbf{q})\, \dot{q}_j + U(\mathbf{q}), \tag{14}$$

or in terms of the conjugate momenta $\mathbf{p} \equiv \mathbf{M}(\mathbf{q}) \cdot \dot{\mathbf{q}}$,

$$H(\mathbf{q}, \mathbf{p}) = \tfrac{1}{2} \sum_{ij} p_i M^{-1}_{ij}(\mathbf{q})\, p_j + U(\mathbf{q}). \tag{15}$$

To be sure, most off-diagonal terms in the kinetic energy will be identically zero; but nonzero, configuration-dependent terms will arise, e.g., when i and j represent two Euler angles of the same molecule. The accelerations $\ddot{q}_k$ do not in general obey simple Newton's equations (Eq. (4)), but the motion of the system can be computed by solving Hamilton's equations for $\dot{p}_k$ and $\dot{q}_k$:

$$\dot{q}_k = \sum_j p_j M^{-1}_{kj}(\mathbf{q}), \tag{16a}$$

$$\dot{p}_k = -\frac{1}{2} \sum_{ij} p_i p_j \frac{\partial}{\partial q_k} M^{-1}_{ij}(\mathbf{q}) - \frac{\partial}{\partial q_k} U(\mathbf{q}), \tag{16b}$$

or, in the special case of rigid-body molecules, coupled Newton–Euler equations [8].

In applying the mass tensor method to a system whose ordinary dynamics is described by the Hamiltonian of Eq. (15), we wish to know to what extent the mass tensor may be modified without affecting the system's equilibrium properties, i.e., without affecting the equilibrium microcanonical probability density, $\rho(\mathbf{q})$, in configuration space. If the system's total energy is E, this density can be obtained by integrating the phase space density, $\delta[H(\mathbf{q}, \mathbf{p}) - E]$, over all the momenta.

$$\rho(\mathbf{q}) \equiv \int_{-\infty}^{\infty} dp^N \, \delta[H(\mathbf{q}, \mathbf{p}) - E] \Big/ \int dq^N \int_{-\infty}^{\infty} dp^N \, \delta[H(\mathbf{q}, \mathbf{p}) - E]$$

$$= \text{const} \mid \mathbf{M}(\mathbf{q}) \mid^{1/2} \cdot [E - U(\mathbf{q})]^{(N-2)/2}. \tag{17}$$

It can be seen that $\rho(\mathbf{q})$ depends on the mass tensor only through the determinant $\mid \mathbf{M}(\mathbf{q}) \mid$. Correct sampling of configuration space will therefore be preserved by any modification of $\mathbf{M}(\mathbf{q})$ which leaves $\mid \mathbf{M}(\mathbf{q}) \mid$ the same function of the coordinates $\mathbf{q}$ as it was in the original system.

As an example of such a modification, consider again a system of rigid-body molecules. The ordinary dynamics of this system involves a mass tensor of the form

$$M_{ij}(\mathbf{q}) = \sum_{kl=1}^{N} T_{ki}(\mathbf{q}) \, T_{lj}(\mathbf{q}) \, I_{kl} \, , \tag{18}$$

where $\mathbf{I}$ is a constant diagonal matrix of principal inertia moments and molecule masses, and $\mathbf{T}(\mathbf{q})$ is an Euler-angle-dependent, nonorthogonal transformation matrix from time derivatives of the Euler angles to angular velocities about the molecules' principal axes. Correct sampling of configuration space would be preserved if $\mathbf{I}$ were replaced by an arbitrary positive-definite, constant, symmetric matrix $\mathbf{I}'$ (more generally, $\mathbf{I}'$ could be a function of $\mathbf{q}$, so long as its determinant was not). A suitable $\mathbf{I}'$ for slowing down fast motions and speeding up slow ones could be obtained from the instantaneous or time-averaged matrix of second derivatives of U with respect to infinitesimal rotations (about the molecules' principal axes) and translations.

A rather different reason for considering a variable mass tensor, even for systems whose ordinary dynamics is described by a constant, diagonal mass, is to avoid the obsolescence of the mass tensor which inevitably results when a system with a fixed mass tensor moves out of that part of configuration space in which the mass tensor was calculated. The obvious solution to this problem—i.e., to periodically update or recalculate the mass tensor on the basis of current force constant information—while it might work well in practice, would introduce a subtle time-dependence into the Hamiltonian, and thus in principle might lead to statistically incorrect sampling of configuration space. This difficulty could be resolved by

using a mass tensor which was an appropriately chosen function of the present configuration only, but not of time or of past configurations. Further numerical and theoretical work is needed to determine whether such a "memoryless" mass tensor (which would probably be more costly to use per time step than a periodically updated one) is indeed necessary to sample configuration space correctly; and if not, what updating scheme is best. It should perhaps be noted that most efficient methods of function minimization [1, 2] do have memory; they make use of curvature information gathered during previous iterations.

If a memoryless definition for the mass tensor turns out to be necessary, it would probably be best to make the mass tensor a simply calculable, piecewise-constant function of $\mathbf{q}$, defined on a rather coarse mesh of cells in configuration space. The trajectory could then be computed by Newton's equations except during its rather infrequent encounters with cell boundaries.

ACKNOWLEDGMENTS

I thank Aneesur Rahman for helpful discussions of the significance of the instantaneous force constant matrix, Scott Kirkpatrick and Ralph Willoughby for advice on sparse matrix techniques, and Philip Wolfe for discussions of function minimization methods.

REFERENCES

1. R. FLETCHER AND M. J. D. POWELL, *Comput. J.* **6** (1963), 163.
2. S. L. S. JACOBY, J. S. KOWALIK, AND J. T. PIZZO, "Iterative Methods for Nonlinear Optimization Problems," Chap. 5, Prentice-Hall, Englewood Cliffs, N.J., 1972.
3. ANEESUR RAHMAN, private communication.
4. J. K. REID (Ed.), "Large Sparse Sets of Linear Equations," Proceedings Oxford Conference, Academic Press, London, 1970.
5. D. J. ROSE AND R. A. WILLOUGHBY (Eds.), "Sparse Matrices and their Applications," 1971 Symposium Proc. IBM Watson Research Center, Yorktown Heights N.Y., Plenum Press, New York, 1972.
6. ALAN GEORGE, *SIAM J. Numer. Anal.* **10** (1973), 345.
7. C. W. GEAR, Argonne National Laboratory Report No. ANL-7126, 1966.
8. A. RAHMAN AND F. H. STILLINGER, *J. Chem. Phys.* **55** (1971), 3336.
9. C. H. BENNETT, in "Diffusion in Solids: Recent Developments," (J. J. Burton and A. S. Nowick, Eds.), Academic Press, New York, 1975.